Battery Health Prognosis: Discharging Capacity Prediction at All Operating Voltage Levels

Zhao, Chunyang; Andersen, Peter Bach; Træholt, Chresten; Hashemi, Seyedmostafa

Published in:
Proceedings of 2023 IEEE Power & Energy Society General Meeting (PESGM)

Link to article, DOI:
10.1109/PESGM52003.2023.10252691

Publication date:
2023

Document Version
Publisher's PDF, also known as Version of record

Battery Health Prognosis: Discharging Capacity Prediction at All Operating Voltage Levels

Chunyang Zhao, Peter Bach Andersen, Chresten Træholt, Seyedmostafa Hashemi
Department of Wind and Energy Systems
Technical University of Denmark
Kongens Lyngby, Denmark
chuzh@dtu.dk, petb@dtu.dk, ctra@dtu.dk, shtog@dtu.dk

***Abstract*—The battery energy storage system is an essential component in the modern energy system with the development of renewable energy, transportation electrification, and carbon-neutral goals. Battery degradation has been the most challenging issue of energy storage. This work presents a data-driven battery degradation model powered by long short-term memory (LSTM) recurrent neural network (RNN). Utilizing the battery dataset with more than 100 batteries exposed to different operations, the proposed model gives a precise prediction of full-discharge capacity and internal resistance (IR) with the root-mean-square error (RMSE) of 0.008 Ah and 0.00017 Ohm in 100 cycles, respectively. Instead of a single capacity or state of health (SOH) value projection, our model predicts the full-discharge capacity-voltage trajectory of the following cycles, addresses the capacity and energy content in different voltage ranges, and improves the accuracy and applicability of the SOH prognosis in industrial applications.**

***Index Terms*—state of health, data-driven prognosis, battery degradation modeling, battery health indicator**

I. Introduction

Batteries are of vital importance with the increasing demand for transportation electrification and energy storage in power systems [1]. Battery aging, known as degradation, is one of the biggest concerns of battery applications. Battery degradation leads to deteriorating performance regarding energy storage, power provision, energy efficiency, etc. During the inevitable degradation process, non-linear performance deterioration is observed, and the battery state of health (SOH) is hard to measure or predict. The inherent battery aging relates to the loss of lithium inventory and active electrode materials, which leads to capacity fade and power fade of battery performance [2]. Addressing the physical transformation and chemical reaction causing the degradation, correlating the battery degradation with the usage of the battery is one of the most viable approaches in this field [3].

The early lithium-ion battery aging test is carried out at NASA Ames research center on 18650 batteries [4]. After 15 years of advancement of battery aging tests, around one thousand cells were tested and published over the world, which became the main resource for degradation research [5]. The operating conditions of the battery cycling, including temperature, current rate (C-rate), and state of charge (SOC), are controlled regarding selected independent factors, and the current, voltage, IR, and temperature of the batteries are recorded over time. Some works test a group of battery cells under the same duty profile to investigate the general degradation behavior and inherent cell-level discrepancy. For example, a group of 48 Nickel Manganese Cobalt is cycled under the same duty profile [6]. Other research focuses on diverse battery duty profile aging tests to address the usage-induced degradation discrepancy. For instance, to investigate the aging performance of batteries under fast charging, the duty profiles of various charging C-rates up to 8C are applied on 124 lithium iron phosphate batteries [7]. To reveal the battery aging performance under random operating conditions, 77 batteries are cycled in fixed or randomized policies, where the C-rate of 1C to 3C are implemented [8]. Overall, the increasing amount of accessible battery aging data is observed, and higher quality of recording and the innovative design of duty profiles are implemented, which promotes the battery degradation research substantially.

Various approaches to degradation modeling are practiced to track and predict the battery degradation performance [9]. The model-based, data-driven, and hybrid approaches are the main three categorizations for degradation modeling [10]. The model-based approach includes the electrochemical model, the equivalent circuit model, the empirical model, etc. To reduce the complexity of modeling and to utilize the abundant battery aging dataset, the data-driven approaches demonstrate the strength of degradation prognosis in recent years. Regression methods are implemented in the degradation research broadly, including lasso and elastic net regression, support vector regression, gaussian process regression, etc. [7], [11], [12].

Addressing the long-term degradation trend and short-term fluctuations, various machine learning methods are built on the decomposition results of degradation trajectories [13]. It enhances the model performance from the capacity characteristic of the battery testing records, without knowing the forming process of capacity at different charging/discharging stages. Recently, LSTM neural network shows great potential for long-term prediction, especially in the field of battery degradation [14]. Various designs such as neural network structure, feature selection, and dropout techniques are implemented for better model performance [15]. It is also combined with other

This work is supported by the Danish project "BOSS: Bornholm smart-grid secured by grid-connected battery systems" co-founded by Danish Energy Technology Development and Demonstration Program (EUDP) contract no.64018-0618.

methods such as ensemble learning, transfer learning, and Monte Carlo methods [16], [17]. The battery accuracy of the model evaluation parameters is quantified by RMSE, mean absolute error (MAE), etc. Previously, one or more values are selected to be the key indicator of capacity degradation. For instance, the full-discharge battery capacity, SOH, IR, etc. However, the aforementioned indicators are highly condensed parameters for degradation description, which is insufficient to describe the complex process and states of battery degradation.

In this work, we expand the battery degradation indicator to a series of capacities at different voltage levels during the discharge process combined with IR to better describe the battery health state. The LSTM machine learning algorithm is used to address the battery life prediction in different operation conditions, which is a good fit for long-term degradation behavior and short-term battery performance fluctuation. The selected battery dataset includes the battery life from hundreds to thousands of cycles, which are grouped in training and testing datasets arbitrarily. Conventional SOH indicators like full-discharge capacity and IR can be precisely predicted, and the battery state of energy at different voltages can be extracted by the novel SOH indicators.

The paper is organized as follows. The recent progress and challenges of battery degradation prognosis are presented in the introduction section. In Section II, the dataset used for modeling is introduced. The LSTM neural network structure and model evaluation parameters are presented in Section III. The details of the data-driven modeling are presented in Section IV. The model results are presented by conventional indicators and our novel indicators in Section V. Finally, the challenge and opportunity of the proposed degradation prognosis framework are discussed in Section VI. Section VII concludes our work.

II. Battery Aging Data

Capturing the long-term battery degradation performance is a time-consuming task, especially with the increasing lifetime of modern lithium-ion battery cells. Therefore, it is essential to run the batteries in a controlled environment from the beginning of life to the end of life, which normally takes from months to years. The battery dataset from the work of [7] is used in this work, consisting of 124 commercial lithium iron phosphate (LFP) degradation testing results published in 2019. The batteries are cycled in the 30 °C with various combinations of fast-charging policies with the combination of different charging C-rates. The discharging process of all the batteries is carried out at 4C, which gives a good reference for the full-discharge capacity in each cycle. The batteries are cycled at least to 80% of the nominal 1.1Ah discharge capacity, which is defined as the end of life (EOL). As shown in Fig. 1, The EOL ranges from a few hundred cycles to more than two thousand cycles. The initial full-discharge capacity tested by the 4C constant current is around 1.05 Ah, and the test finishes up to 0.7Ah for the short-life batteries. As shown in Fig. 2, the IR is presented along the battery cycle count. The IR is tested by the pulse current at 80% SOC during the charging

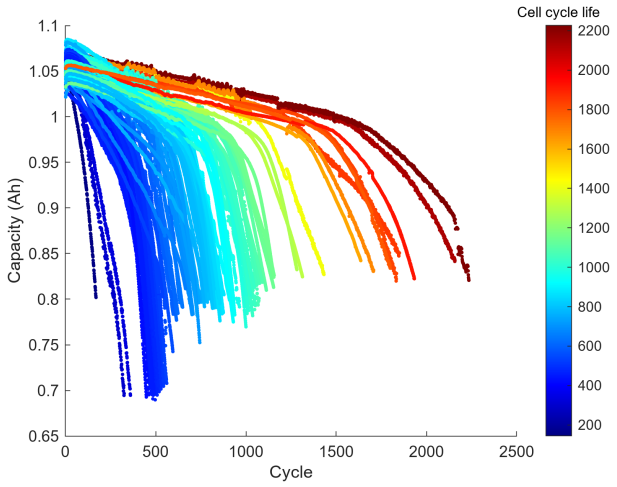

Fig. 1: Degradation performance of the batteries in the dataset: full-discharge capacity development over cycle count

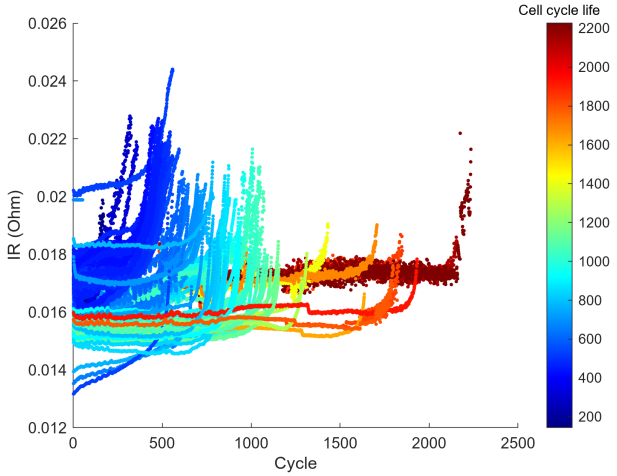

Fig. 2: Degradation performance of the batteries in the dataset: IR development over cycle count

process, which shows a correlation with the full-discharge capacity. Though the batteries are cycled in a temperature chamber set at 30°C, the temperature measurement on the surface of the battery changes constantly caused by the energy conversion loss and the heat effect of the current. However, the temperature measurement is hard to use directly in the modeling, since the cell temperature is influenced by internal causes such as the IR development, C-rate, etc., and external causes such as the characteristic of the temperature chamber, battery placement, sensor accuracy, etc.

III. Methodology

A. Structure of LSTM

With the increasing lifetime of lithium-ion batteries, it is essential to capture the long-term degradation development together with short-term fluctuation by contemporary algorithms. The RNN is a powerful deep-learning tool with great potential for tasks involving sequential inputs. However, the gradients

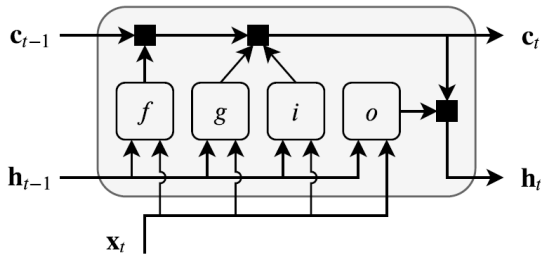

Fig. 3: The data flow of LSTM cell at time step t [18]

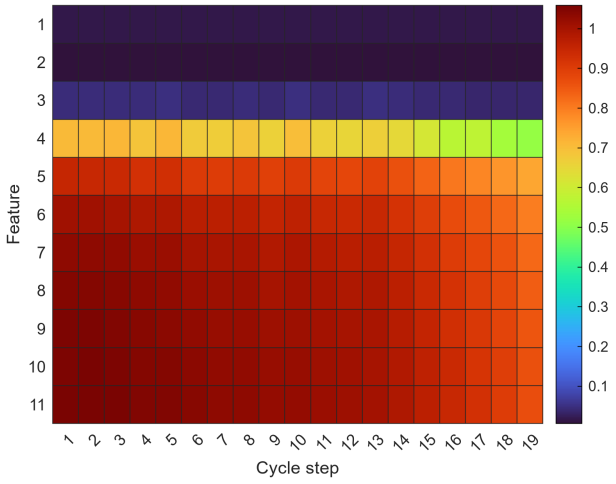

Fig. 4: Illustration of data and features for modeling: IR (feature No.1) + 10 discharge capacity at different voltages (feature No.2-11) with cycle step of 100 cycles

of RNN tend to explode or vanish during the backpropagation training process, which hinders the long-term memory of the model. The LSTM is a type of RNN equipped with both long-term and short-term memory [19], as the LSTM unit allows the gradients to be passed unchanged during the training. As shown in Fig. 3, the data flow in the LSTM cell from time step $t-1$ to t is presented. The input includes the cell state at time step $t-1$ (c_{t-1}), the hidden state at time step $t-1$ (h_{t-1}), and the input series at time step t (X_t). The outputs are the cell state (c_t) and hidden state (h_t) at the time step t, which are passed to the next LSTM cell. In this work, The X_t are the features extracted from the battery operation records. During the training process, the input weights, recurrent weights, and biases are learned. The gate design gives the LSTM network the ability to have long-term memory. As shown in Fig. 3, the *f*, *g*, *i*, and *o* represent the forget gate, cell candidate, input gate, and output gate, respectively. In the calculation flow, c_t is given by:

$$c_t = f_t \odot c_{t-1} + i_t \odot g_t \tag{1}$$

and the hidden state at time step t is given by:

$$h_t = o_t \odot \sigma_c(c_t) \tag{2}$$

where the $\odot$ denotes the element-wise multiplication for vectors, and σ_c denotes the hyperbolic tangent gate activation function. The detailed LSTM architecture and training process can be found at [18], [19].

B. Model evaluation parameters

The RMSE is used to measure the model performance, comparing the difference between the predicted value with the measured value. It is defined as:

$$RMSE = \sqrt{\frac{1}{n}\sum_{j=1}^{n}(y_j - \hat{y}_j)^2} \tag{3}$$

where the $\hat{y}_j$ is the estimation value of item j, y_i is the measurement value of item j, and n is the number of items. To better represent the model performance compared with the scale of the measurement data, the mean absolute percentage error (MAPE) is calculated as:

$$MAPE = \frac{100\%}{n}\sum_{j=1}^{n}\left|\frac{y_j - \hat{y}_j}{y_j}\right| \tag{4}$$

IV. Modeling

With adequate battery aging test resources and a flexible machine learning framework, our model aims at providing a multi-indicator battery health prognosis for battery degradation. The novel indicators we proposed including battery discharge capacity at different voltage levels and IR are the main outputs. Different from the prior capacity prediction works, which only cover the full-discharge capacity, we would like to address the discharge capacity from the fully charged battery to different voltage levels. Specifically, the LFP batteries in the selected dataset have an operation range from 3.5 volts to 2 volts in each constant-current discharging process. As the capacity change is recorded for every 0.0015 volts, there are 1000 capacity measurements in the discharge process. Therefore, we define the capacity feature in our model by the number of capacity measurements, which are measured in the same voltage distance. For instance, 1 capacity feature is the single full-discharge capacity, 10 capacity features are the 10 discharge-capacity records at each 0.015 volts voltage drop from 3.5 volts, and so on.

As shown in Fig. 4, the prepared dataset of 1 IR feature at row No.1 plus 10 capacity features at row No.2 to No.11 with a cycle step of 100 cycles is organized together. The cycle step is the prediction interval defined in our model, which is 100 cycles. In our model, the input is a series of features at any specific cycle step, and the prediction target is the series of features at the cycle step of the furture. The design of the same structure of input and output gives the flexibility of both closed-loop prediction and open-loop prediction. Since 100 cycles are already significant for battery usage, the open-loop prediction approach is used, therefore, the model predicts the battery aging performance in 100 cycles at different stages, and prior degradation performance is memorized. As there are 124 batteries in the dataset, the first 90 % of the batteries are used as training datasets and the rest 10% batteries are used as the test datasets, which are 109 and 13 respectively.

Besides capacity records and IR, two other features are considered in the modeling, including the capacity difference and end-of-cycle temperature. The capacity difference is calculated by subtracting the first-cycle capacity records from each following cycle, and the end-of-cycle temperature is the temperature measurement at the end of each full-discharge process. The extra features did not turn out to enhance the model accuracy, which is detailed in the results section.

TABLE I: Model performance evaluated by full-discharge capacity prediction accuracy

Model No.	**Model inputs and performance**		
	No. of Capacity Features	**RMSE**	**MAPE**
1	1	0.00968	0.73%
2	10	0.00804	0.59%
3	100	0.00906	0.71%
4	1000	0.0102	0.76%
5	10[a]	0.00986	0.76%
6	10[b]	0.0144	1.15%

[a]Plus capacity difference features
[b]Plus capacity difference and end-of-cycle temperature features.

TABLE II: Model performance evaluated by IR prediction accuracy

Model No.	**Model inputs and performance**		
	No. of Capacity Features	**RMSE**	**MAPE**
1	1	1.65E-04	0.76%
2	10	1.70E-04	0.85%
3	100	3.26E-04	1.77%
4	1000	4.97E-04	2.80%
5	10[a]	1.78E-04	0.87%
6	10[b]	3.22E-04	1.66%

[a]Plus capacity difference features
[b]Plus capacity difference and end-of-cycle temperature features.

V. Results

A. Results evaluated in conventional indicators

Conventionally, the degradation model is evaluated by the prediction accuracy of the full-discharge capacity and IR, which are covered by our model. As shown in Table I and Table II, the model performance is evaluated by full-discharge and IR prediction accuracy, respectively. The RMSE and MAPE are the average values of all the testing datasets. There are six models presented, and the sensitivity analysis is carried out by the difference in the model inputs. From model No.1 to No.4, different No. of capacity, features are given from 1 to 1000. Model No.2 with 10 capacity features gives the lowest RMSE and MAPE for full-discharge capacity prediction and Model No.1 wins for IR prediction accuracy. Therefore, the increasing amount of capacity information at different voltages during the discharge process improves the modeling performance of full-discharge capacity prediction at the beginning, and the modeling performance decreases when there is too much information during the discharge process, which may shift the focus of model performance from predicting the full-discharge capacity to the multi-voltage capacity. However, increasing information on the discharge capacity at different voltage levels does not increase the performance of the IR prediction, the potential reason might be that the LSTM is a very flexible method and can fit IR development pretty well already with the full-discharge capacity feature, etc. The model performance on all the testing datasets is presented by the histogram of RMSE and MAPE in Fig. 5. And further-step trajectory predictions are demonstrated in Fig. 6, which shows precise prediction results on fully-discharge capacity and IR. Besides the feature combination of IR and discharge capacity, Model No.5 and Model No.6 are used to investigate the supplement features of capacity difference and end-of-cycle temperature. However, the additional feature does not improve the model's performance in the conventional evaluation framework.

B. Results evaluated in novel indicators

As shown in Fig. 7, the model accurately gives the prediction of the full discharge trajectory of the future cycle step, and the development of the discharge performance of the test case is presented. Instead of full-discharge capacity, 1000 points of discharge capacity are predicted from 3.5 volts to 2 volts. The red smooth lines are the measurement records, and the noisy lines in other colors are the predictions. The test case has a cycle life of 900 cycles, and the prediction is made from the 6th cycle step to the 9th cycle step, which is from 600 cycles to 900 cycles. In summary, the model shows a great performance for degradation prognosis during the whole discharge process at different voltage levels.

VI. Discussion

Overall, the model proposed in this work gives a novel scope of degradation prognosis. Traditionally, various single values are used to describe the battery SOH such as full-discharge capacity, IR, remaining useful life, etc. However, degradation is a complex process and is hard to be described by single values. Another limitation of the conventional capacity prediction is the neglect of voltage during the charging and discharging process. In most applications, the remaining useful power and energy of the battery are the most important information rather than capacity. As the voltage is changing during the battery discharge process, it is impossible to estimate the remaining energy accuracy without the voltage information. With our novel indicator of the full capacity-voltage information during discharge, the remaining energy can be easily estimated by the integration of capacity on voltage. Furthermore, the accessible energy from any voltage range or SOC range can also be accurately calculated by definite integrations.

VII. Conclusion

In this work, the data-driven degradation model powered by LSTM is proposed for degradation prognosis by predicting the capacity-voltage trajectories for the full-discharge process at different stages. Besides accurately forecasting the capacity-voltage relation, the LSTM model gives precise predictions on full-discharge capacity and IR. Our best model achieves

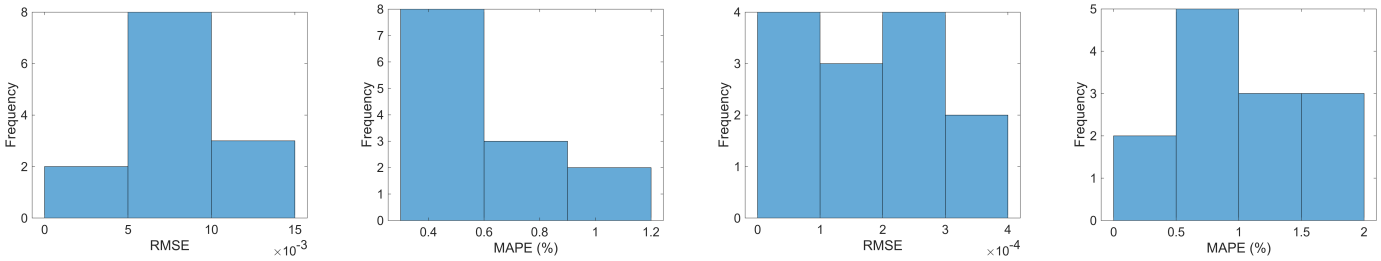

(a) Capacity prediction: RMSE (b) Capacity prediction: MAPE (c) IR prediction: RMSE (d) IR prediction: MAPE

Fig. 5: Model performance on testing datasets

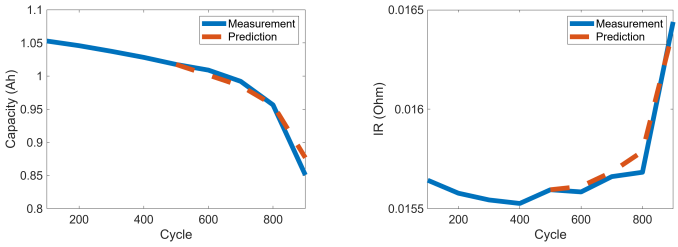

(a) Capacity prediction (b) IR prediction

Fig. 6: Degradation prognosis: trajectories of full-discharge capacity and IR

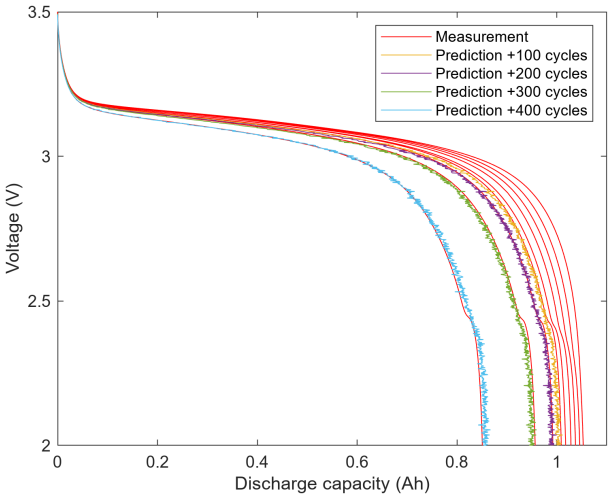

Fig. 7: Degradation prognosis: discharge capacity at all voltage levels during the discharge process

0.008 Ah RMSE and 0.59% MAPE on capacity prediction, and 0,00017 Ohm RMSE and 0.85% MAPE on IR prediction in 100 cycles. Besides the conventional SOH indicators, our model depicts the useful discharge capacity at different voltage levels of the full discharge process, which improves the SOH indicators significantly. The precise prediction of the novel SOH indicators can be used to estimate the available capacity and energy at any discharge voltage range of various applications in the future.

REFERENCES

[1] C. Zhao, S. Hashemi, P. B. Andersen, and C. Traholt, "Data-driven State of Health Modeling of Battery Energy Storage Systems Providing Grid Services," in *2021 11th International Conference on Power, Energy and Electrical Engineering (CPEEE)*, no. 64018, pp. 43–49, IEEE, 2 2021.

[2] C. R. Birkl, M. R. Roberts, E. McTurk, P. G. Bruce, and D. A. Howey, "Degradation diagnostics for lithium ion cells," *Journal of Power Sources*, vol. 341, pp. 373–386, 2017.

[3] X. Han, L. Lu, Y. Zheng, X. Feng, Z. Li, J. Li, and M. Ouyang, "A review on the key issues of the lithium ion battery degradation among the whole life cycle," *eTransportation*, vol. 1, p. 100005, 2019.

[4] B. Saha and K. Goebel, "Battery Data Set," 2007.

[5] G. dos Reis, C. Strange, M. Yadav, and S. Li, "Lithium-ion battery data and where to find it," *Energy and AI*, vol. 5, p. 100081, 9 2021.

[6] W. Li, N. Sengupta, P. Dechent, D. Howey, A. Annaswamy, and D. U. Sauer, "One-shot battery degradation trajectory prediction with deep learning," *Journal of Power Sources*, vol. 506, p. 230024, 9 2021.

[7] K. A. Severson, P. M. Attia, N. Jin, N. Perkins, B. Jiang, Z. Yang, M. H. Chen, M. Aykol, P. K. Herring, D. Fraggedakis, M. Z. Bazant, S. J. Harris, W. C. Chueh, and R. D. Braatz, "Data-driven prediction of battery cycle life before capacity degradation," *Nature Energy*, vol. 4, pp. 383–391, 5 2019.

[8] J. Lu, R. Xiong, J. Tian, C. Wang, C.-W. Hsu, N.-T. Tsou, F. Sun, and J. Li, "Battery degradation prediction against uncertain future conditions with recurrent neural network enabled deep learning," *Energy Storage Materials*, vol. 50, pp. 139–151, 9 2022.

[9] C. Zhao, P. B. Andersen, C. Traeholt, and S. Hashemi, "Data-driven Cycle-calendar Combined Battery Degradation Modeling for Grid Applications," in *2022 IEEE Power & Energy Society General Meeting (PESGM)*, pp. 1–5, IEEE, 7 2022.

[10] X. Hu, L. Xu, X. Lin, and M. Pecht, "Battery Lifetime Prognostics," 2 2020.

[11] R. R. Richardson, M. A. Osborne, and D. A. Howey, "Battery health prediction under generalized conditions using a Gaussian process transition model," *Journal of Energy Storage*, vol. 23, pp. 320–328, 6 2019.

[12] X. Feng, C. Weng, X. He, X. Han, L. Lu, D. Ren, and M. Ouyang, "Online State-of-Health Estimation for Li-Ion Battery Using Partial Charging Segment Based on Support Vector Machine," *IEEE Transactions on Vehicular Technology*, vol. 68, pp. 8583–8592, 9 2019.

[13] K. Liu, Y. Shang, Q. Ouyang, and W. D. Widanage, "A Data-Driven Approach with Uncertainty Quantification for Predicting Future Capacities and Remaining Useful Life of Lithium-ion Battery," *IEEE Transactions on Industrial Electronics*, vol. 68, no. 4, pp. 3170–3180, 2021.

[14] Y. Zhang, R. Xiong, H. He, and M. G. Pecht, "Long short-term memory recurrent neural network for remaining useful life prediction of lithium-ion batteries," *IEEE Transactions on Vehicular Technology*, vol. 67, pp. 5695–5705, 7 2018.

[15] K. Park, Y. Choi, W. J. Choi, H. Y. Ryu, and H. Kim, "LSTM-Based Battery Remaining Useful Life Prediction with Multi-Channel Charging Profiles," *IEEE Access*, vol. 8, pp. 20786–20798, 2020.

[16] Z. Deng, X. Lin, J. Cai, and X. Hu, "Battery health estimation with degradation pattern recognition and transfer learning," *Journal of Power Sources*, vol. 525, p. 231027, 3 2022.

[17] H. Zhang, G. Niu, B. Zhang, and Q. Miao, "Cost-Effective Lebesgue Sampling Long Short-Term Memory Networks for Lithium-ion Batteries Diagnosis and Prognosis," *IEEE Transactions on Industrial Electronics*, 2021.

[18] "Long Short-Term Memory Networks - MATLAB & Simulink - MathWorks Nordic."

[19] S. Hochreiter and J. Schmidhuber, "Long Short-Term Memory," *Neural Computation*, vol. 9, pp. 1735–1780, 11 1997.